Opt Rev (2015) 22:802–808
DOI 10.1007/s10043-015-0136-z

REGULAR PAPER

Enhancing resolution of single-pixel imaging system

Dongfeng Shi[1] · Jian Huang[1] · Feng Wang[1,2,3] · Kaifa Cao[1] · Kee Yuan[1] · Shunxing Hu[1] · Yingjian Wang[1,2]

Received: 25 March 2015 / Accepted: 6 August 2015 / Published online: 19 August 2015

Abstract In this paper, we propose a subpixel-shifted method to overcome the limitations on the resolution of an image obtained from single-pixel imaging system. In the proposed method, modulation system is moved by sub-integer low grid units, and new information contained in each shifted low grid area can be exploited to obtain a high-resolution image. The front and back modulation single-pixel imaging systems are analyzed. Based on the shifted and point spread function parameters, this method using compressed sensing algorithm can overcome the limitative resolution generated by the modulation system pixel size and transmission effect to get high-resolution image. Finally, the machining experiment results prove the effective of the proposed method.

Keywords Imaging system · Image enhancement · Super-resolution

✉ Kee Yuan
keyuan@aiofm.ac.cn

Dongfeng Shi
dfshi@aiofm.ac.cn

[1] Key Laboratory of Atmospheric Composition and Optical Radiation, Anhui Institute of Optics and Fine Mechanics, Chinese Academy of Sciences, Hefei 230031, China

[2] University of Science and Technology of China, Hefei 230026, China

[3] State Key Laboratory of Pulsed Power Laser Technology, Electronic Engineering Institute, Hefei 230037, China

1 Introduction

Single-pixel imaging system [1–13] is a prospective approach for the development of the imaging system. A single-pixel imaging system can render the image of an object using just a single-pixel detector without a scanning device. This is particularly important when the matrix detector is expensive or unable to be achieved. A single-pixel imaging system with other devices can yield different kinds of images. For example, single-pixel imaging system with a point detector array and a dispersive element connected to it can create three-dimensional [1] or multi-spectral or hyper-spectral images of an object [2, 3], whereas, with a fast response detector and an ultra-short pulse source, it can reconstruct the fine three-dimensional structure of an object [4, 5].

Single-pixel imaging system can be roughly divided into two models: (a) the front modulation model and (b) the back modulation model. Modulated information is added in different paths, which is the difference between the two models. For the front modulation model, the modulated information is added in the transmission system; for the back modulation model, it is added in the receiving system. Ghost imaging (GI) [1, 5–8] is a typical example of the front modulation model of single-pixel imaging system. When the modulated information is added in the receiving system [4], the back modulation model which is a more flexible single-pixel imaging system can be built. In this system, the active mode works when the laser source works, while the passive mode works when the imaging depends on background radiation. The photon counting active back modulation system is built to obtain the three-dimensional scene [4]. The characterization of the passive back modulation system is studied in this paper [9].

Compressed sensing (CS) algorithm [10] plays a crucial role in single-pixel imaging system. Many types of signals or images can be well approximated by a sparse expansion in terms of a suitable basis. When the number of samples is smaller than the length of the full image or signal, it will involve solving an underdetermined matrix equation. Thus, there will be a huge number of candidate solutions. CS is a strategy to select the best candidate. As a result, CS has become an important research topic, especially in the field of single-pixel imaging. Single-pixel imaging system employs CS not only to reduce the number of the samples, but also improve the quality of the recovered image [2, 3, 11–13]. With the development of photoelectron technology and CS algorithms, single-pixel imaging system now has broad application prospects.

For any imaging system, the resolution of an obtained image is a principal factor determining its quality [14, 15]. In the case of the front modulation model of single-pixel imaging system, the resolution of an image is limited by the size of speckle, which is determined by the pixel size of the modulation system and the transmission effect in the source-to-scene path (e.g., aberration of transmission system, diffraction limit, and turbulence), whereas, for the back modulation model, it is determined by transmission effect in the scene-to-detector path (e.g., aberration of receiving system, diffraction limit, and turbulence) apart from the pixel size of the modulation system. The transmission effect can be described as the degradation by the point spread function (PSF) of the system which describes the response of an imaging system to a point source or point object. In functional terms, it is the spatial domain version of the transfer function of the imaging system. There is a big demand for high-resolution images, because the additional detail they offer is important for analysis in many applications. In order to obtain a high-resolution image, the conventional technology depends on reducing the modulation system pixel size and eliminating transmission effect. Nevertheless, the cost for high-precision optics system and improvements in the modulation system based on conventional technology may be too high. In order to overcome this problem, traditional array imaging system uses a resolution enhancement approach called super-resolution (or high-resolution) technology in many literatures [14, 15], which is based on signal processing techniques. At present, the methods [14, 15] based on the multi-frame low-resolution images are widely used for low-resolution charge-coupled device (CCD) imaging system. The multi-frame low-resolution images must have different subpixel shifts from each other in order to utilize new information to recover a super-resolution (or high-resolution) image. A subpixel-shifted method is employed, which can exploit new information in a low-resolution single-pixel imaging system to obtain super-resolution (or high-resolution) image. In Ref. [16], the authors use the shifted method to get the super-resolution image for the front modulation model single-pixel imaging system, and they ignore the transmission effect. In references [6, 7], the authors employ sample classification based on image sparse character to get the super-resolution image for the front modulation model single-pixel imaging system, and the transmission effect is also ignored. Therefore, the resolution of the recovered image from the above references [6, 7, 16] method is limited by the transmission effect. In Ref. [8], the authors consider the transmission effect to recover the image in the back modulation single-pixel imaging model, but the resolution of the restored image is limited by the pixel size of the modulation system. In this paper, the CS algorithm using the different intensities detected after subpixel shifts and the transmission effect parameters is applied to get a super-resolution (or high-resolution) image. This method can overcome the limitative resolution generated by the modulation system pixel size and transmission effect to get super-resolution (or high-resolution) image. In the remainder of the paper, we describe the method and give the results of our study.

2 Theoretical analysis

In a single-pixel imaging system, the modulation system is a key component. For the front modulation model, when a coherent source of light [17] is employed, a phase modulation device (e.g., ground glass, SLM) as the modulation system can be utilized to add random phase modulation in order to obtain speckle [5], whereas, in the case of an incoherent source or the back modulation model [4, 8, 9], a digital micro-mirror device (DMD) is commonly used as the modulation system. The DMD [18] is an array of individually addressable mirrors that can be selectively oriented to reflect light. TI's new commercial DMD system with an external trigger and 20 kHz of binary modulation speed greatly expands the application of a single-pixel imaging system. In this paper, we suppose that the single-pixel imaging system uses an incoherent source of light and a DMD as the modulation system. Figure 1 shows the two types of single-pixel imaging systems.

For the front modulation model, the light modulated by the DMD is described as matrix containing elements that take either of the values 0 or 1, and then transmits to the scene. At last, the reflected light is collected by a single-pixel detector. The modulated light from the DMD to the scene suffers from interference due to factors, such as aberration of the transmission system, diffraction limit, and turbulence. The evolution process can be expressed by convolution. A mathematical expression describing the imaging process is as follows:

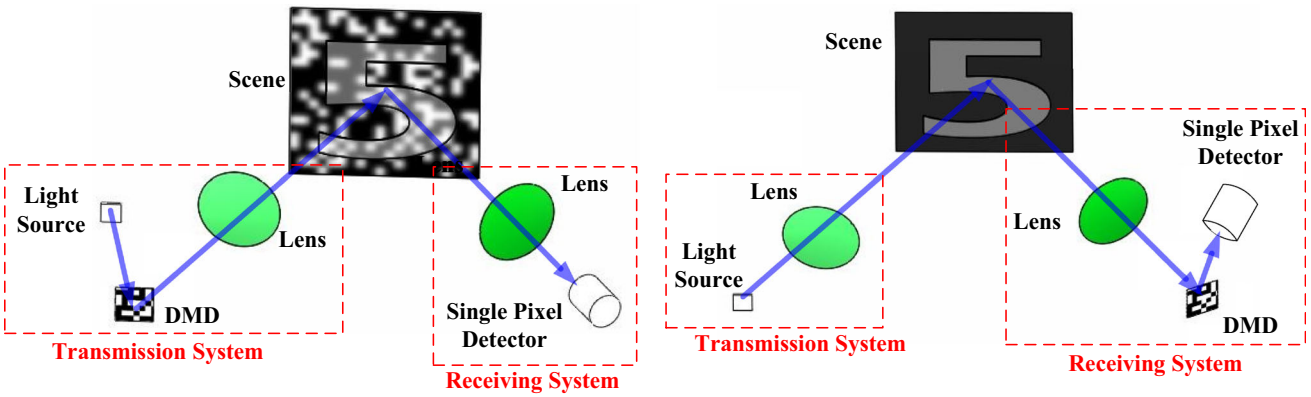

Fig. 1 Two types of single-pixel imaging systems: (*Left*) the front modulation model, (*Right*) the back modulation model

$$i_n = \sum (h * b_n) \cdot p = \sum (h * b_n \cdot p), \tag{1}$$

where n denotes the n-th sample, i is the signal detected by the single-pixel detector, b is the modulation binary matrix, h is the PSF from the interference factors (e.g., aberration of system, diffraction limit, turbulence.), p is the scene matrix, * is the convolution symbol, and $\cdot$ is the Hadamard product symbol. For the sake of recovering the scene matrix, a large number of samples are needed. The mathematical representation can be given as follows:

$$I = HBP, \tag{2}$$

where $I = [i_1; i_2; \ldots; i_n; \ldots]$ is the measured signal matrix, H, B, and P are the matrixes presentation of the PSF, the modulation binary information, and the scene, respectively.

In the case of the back modulation model, the light illuminates the scene, and then the reflected light is modulated by the DMD. Finally, a single-pixel detector detects the light intensity. The reflected light from the scene to the DMD also suffers from interference due to the same factors as the front modulation model. This evolution process can also be expressed by convolution. The imaging process is expressed by a mathematical expression as follows:

$$i'_n = \sum b'_n \cdot (h' * p), \tag{3}$$

Considering the whole sample process, we give the following equation:

$$I' = B'H'P. \tag{4}$$

The symbols have the same meanings as the described earlier. We can see that the two different models of single-pixel imaging system have the similar expression demonstrating the imaging process. The difference between them is the PSF in each case, because of the path difference. The PSF is one of the constraints on the resolution of single-pixel imaging system. The pixel size of the modulation system is another constraint on the resolution of the image.

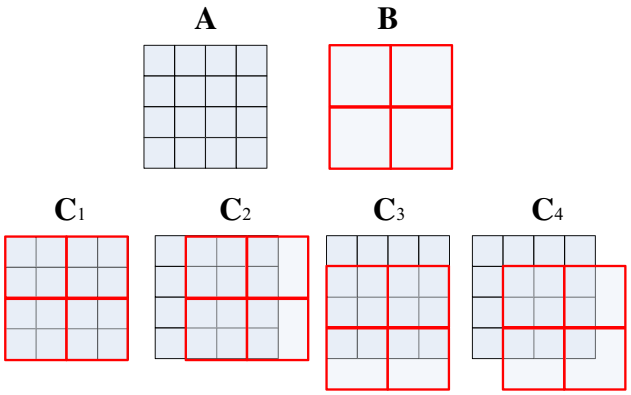

Fig. 2 Illustration of subpixel shift: **a** high-resolution image grid; **b** low-resolution grid determined by single-pixel imaging system; **c1**–**c4** four subpixel shift instances

In Fig. 2a is the high-resolution grid of the scene for the front modulation model or the reflected scene for the back modulation model, and B is the low-resolution grid of the speckle size for the front modulation model or the DMD pixel size for the back modulation model. The resolution of the recovered image is determined by the low-resolution grid (Fig. 2b). This effect is usually modeled as a spatial averaging operator as shown in Fig. 2c1. In order to obtain high-resolution recovered image, signal processing techniques have been a great concern in many areas. If B is shifted by integer low grid units, then each low grid area contains the same information, and thus there is no new information that can be used to reconstruct a high-resolution image. However, if B is shifted by sub-integer low grid units, then each low grid area contains the different information. This principle is shown in the Fig. 2c2–c4. In this case, the new information that is contained in each low grid area can be exploited to obtain a high-resolution image. This sub-integer low grid shift can be achieved by adjusting the DMD. Combining these shifted parameters and sub-integer low grid information, high-resolution

image reconstruction is possible. Now, we rewrite the Eqs. (2) and (4) to contain the shifted information,

$$I = SHBP, \tag{5}$$

$$I' = S'B'H'P, \tag{6}$$

where S and S' are the shifted matrixes. The matrix with ones below (or up) the main diagonal and zeros elsewhere is lower (or upper) shifted matrix. The resolution of the shifted parameters determines the spatial resolution of the recovered image in ideal condition. The 1 and 2 y-shifted matrixes corresponding to shift the matrix one and two pixels along y direction can be expressed as follows:

$$S_{y1} = \begin{bmatrix} 0 & 1 & 0 & 0 & 0 & \cdots & 0 \\ 0 & 0 & 1 & 0 & 0 & \cdots & 0 \\ 0 & 0 & 0 & 1 & 0 & \cdots & 0 \\ 0 & 0 & 0 & 0 & 1 & \cdots & 0 \\ 0 & 0 & 0 & 0 & 0 & \cdots & 0 \\ 0 & 0 & 0 & 0 & 0 & \cdots & 1 \\ 0 & 0 & 0 & 0 & 0 & \cdots & 0 \end{bmatrix}, \; S_{y2} = S_{y1}S_{y1}. \tag{7}$$

According to matrix transpose, the x-shifted matrixes can be achieved [19]. We call this method as subpixel-shifted method (Note that a pixel is denoted by a low grid unit). In the use of reconstruction methods, the characteristics of the PSF are assumed to be known. However, if it is difficult to obtain this information, PSF should be incorporated into the reconstruction procedure. This technology is called blind super-resolution [20]. In this study, we assume that the characteristics of the PSF are known. Now, the parameters S, I, H, B, S', I', H', and B' are known, and consequently the high-resolution image P can be recovered.

Because the number of the samples is smaller than that of the high-resolution image pixels, there are a huge number of candidate solutions. To recover the correct solution, the CS method based on the fact that a vast majority of the nature signals are sparse in some transforms is always used. In this paper, the TV method is utilized to restore the high-resolution image P as follows:

$$\arg\min[\mathrm{TV}(P)] \text{ subject to } I = SHBP, \tag{8}$$

$$\arg\min[\mathrm{TV}(P)] \text{ subject to } I = S'B'H'P. \tag{9}$$

The code employed for compressive sensing was the function tvqc_logbarrier of the l_1-*magic* software package

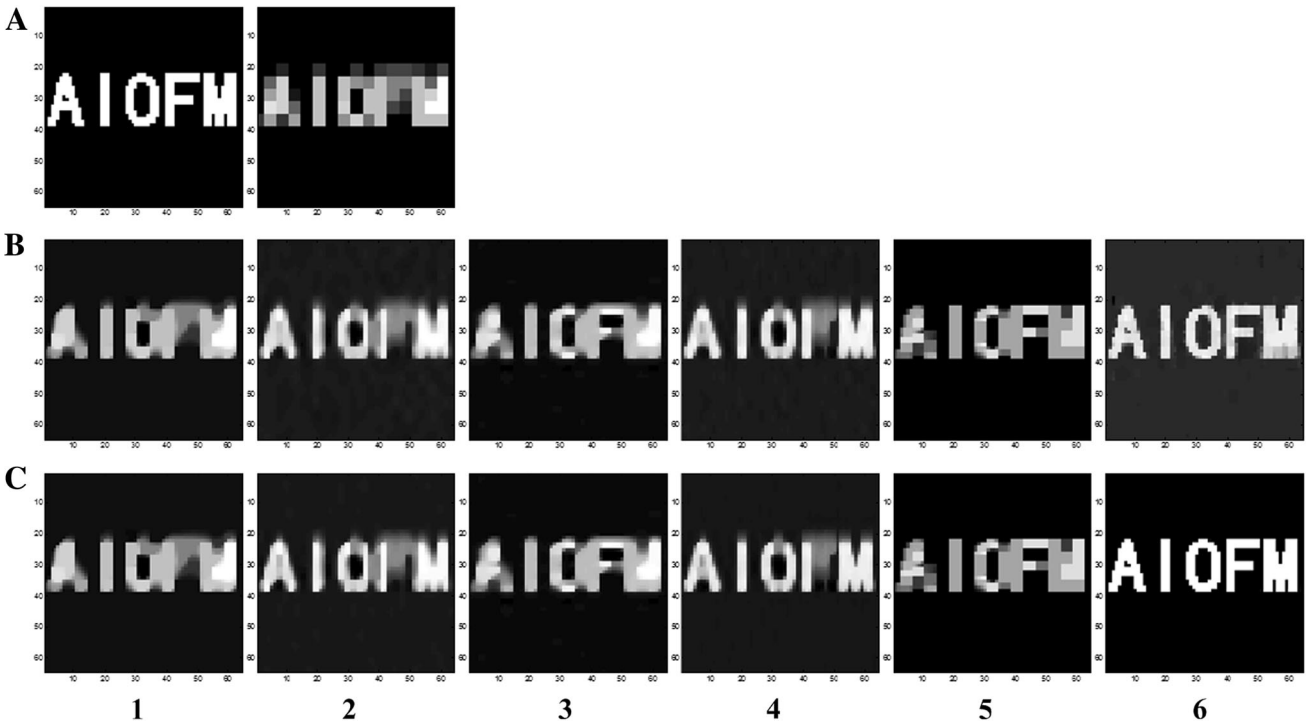

Fig. 3 Experimental results for the first simulation. **b** and **c** are the reconstructed results with a total sampling number of 480 and 960, respectively. **a-1** the original high-resolution scene, **a-2** the low-resolution scene which is determined by the pixel size of the modulation system, **b-1** and **c-1** are the recovered images using the traditional method, **b-2** and **c-2** are the recovered images by shifting the modulation matrix along the x axis, and the step size is the two image pixel size. **b-3** and **c-3** are the recovered images by shifting the modulation matrix along the y axis, and the step size is the two image pixel size. **b-4** and **c-4** are the recovered images by shifting the modulation matrix along the x axis, and the step size is the one image pixel size. **b-5** and **c-5** are the recovered images by shifting the modulation matrix along the y axis, and the step size is the one image pixel size. **b-6** and **c-6** are the recovered images by shifting the modulation matrix along both the x and y axis with one image pixel step size

[21]. In the next section, we will prove the effectiveness of this method through experiments.

3 Computer simulation experiments

The parameter epsilon is equal to 0.05 and other parameters use the default values [21]. Our computer simulation experiments involve two simulations based on the influence of the PSF on imaging. In the first simulation, we assume that the influence of PSF is negligible and can be ignored. The pixel of the modulation system is 16 times larger than the pixel of the imaging scene. In Fig. 3a-1 shows the original 64 × 64 image pixels high-resolution scene. In Fig. 3, a-2 shows the low-resolution scene which is determined by the pixel size of the modulation system. As we have shown in Fig. 2, it is equivalent to the spatial averaging effect. In Fig. 3b, c are the reconstructed results with a total sampling number of 480 and 960, respectively. The same number of samples is used in each of the shifts. In Fig. 3b-1, c-1 are the images recovered using the traditional method, respectively. The results show that the resolution of the restored images obtained using the traditional method is determined by the pixel size of the

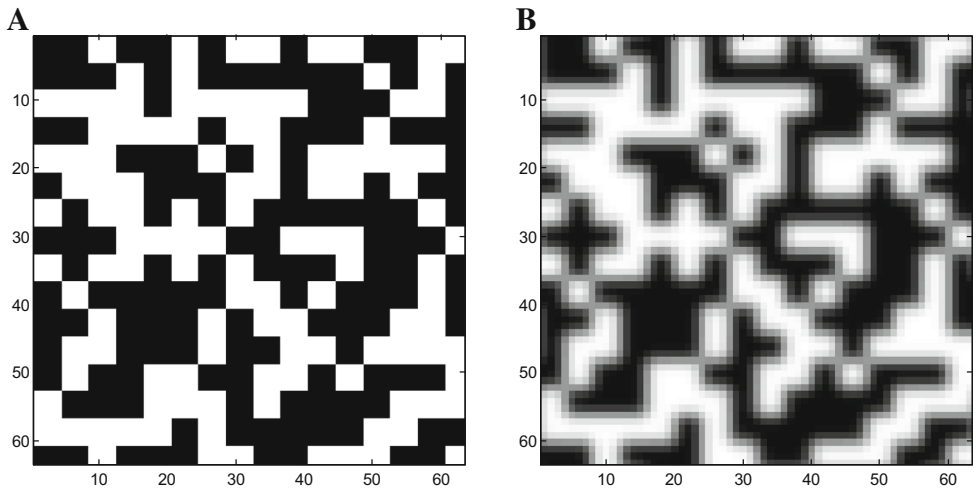

Fig. 4 One binary modulation light example: **a** the original modulation light; **b** the degraded modulation light

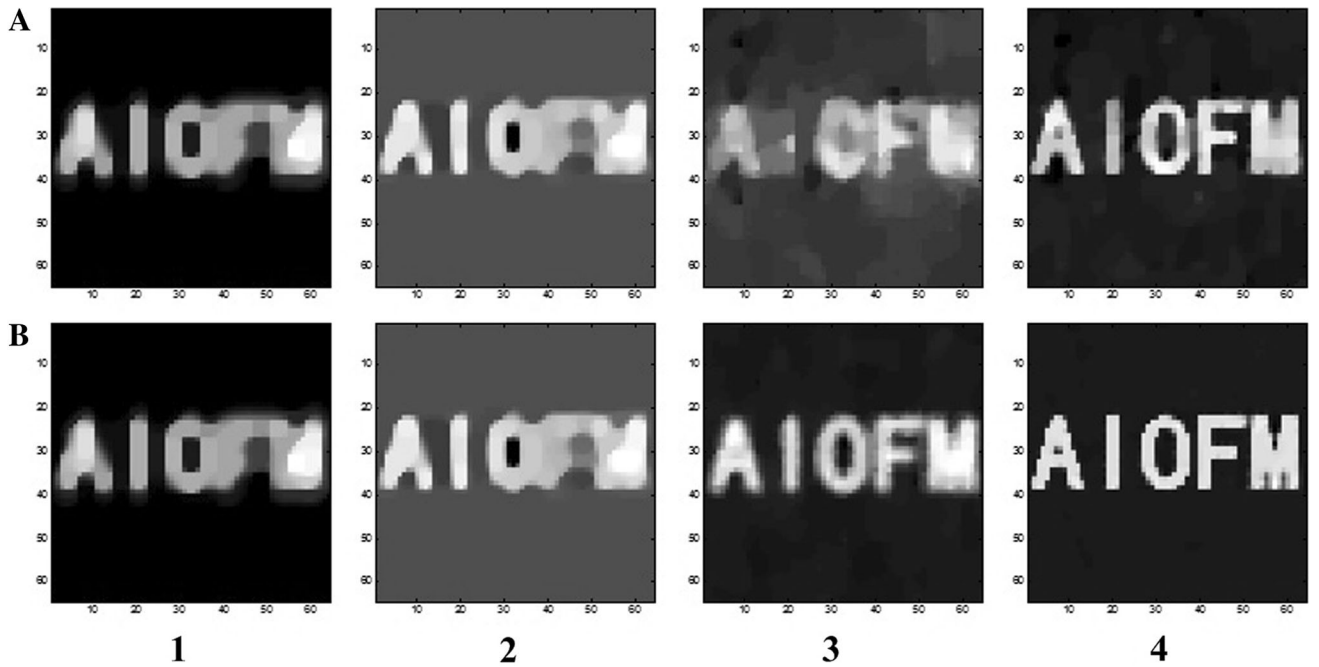

Fig. 5 Experimental results: the *first* and *second rows* are the reconstructed results with the total sampling number of 480 and 960, respectively. 1, 2, 3, and 4 columns are the recovered images in the simulations (a), (b), (c), and (d), respectively

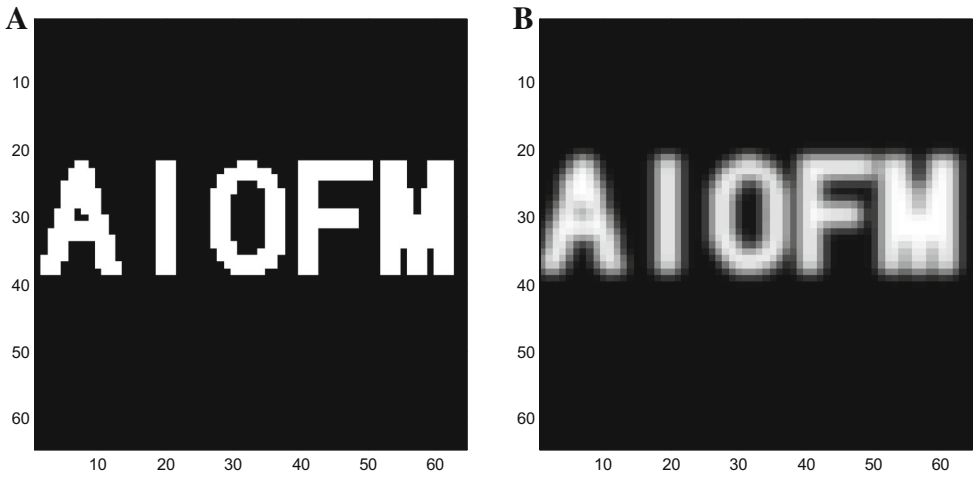

Fig. 6 The example of the degraded scene in the back modulation model: **a** the original scene; **b** the degraded scene

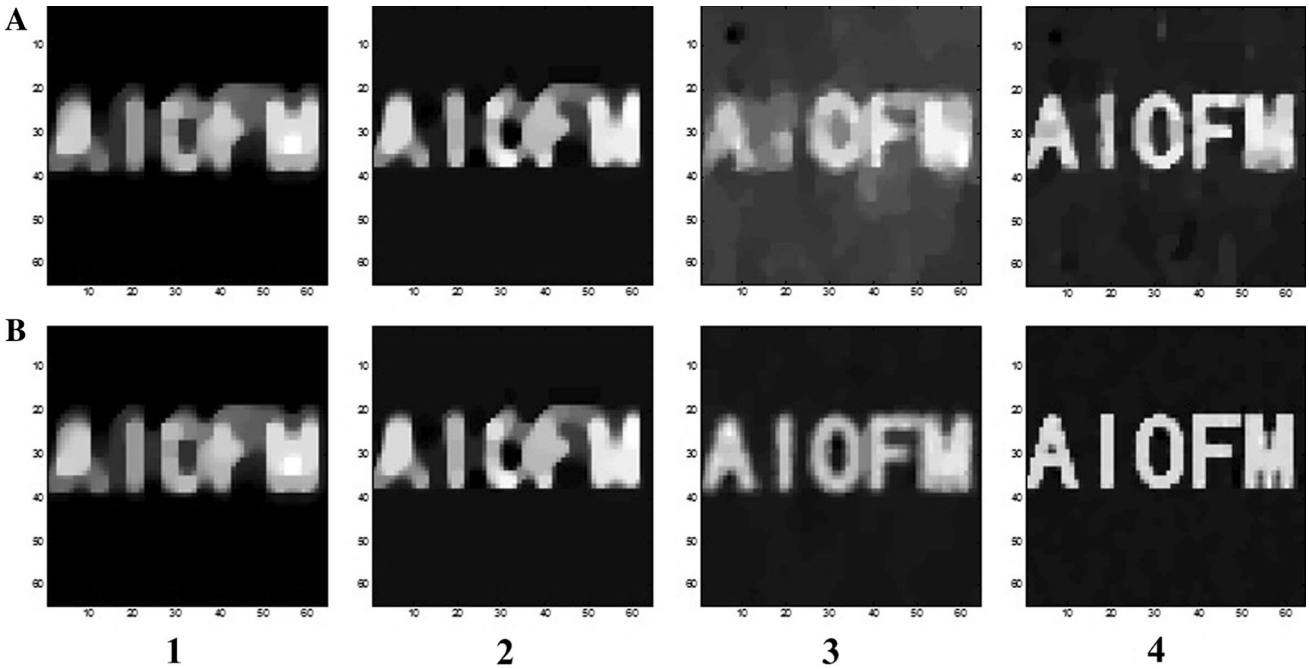

Fig. 7 Experimental results: the *first* and *second rows* are the reconstructed results with the total sampling number of 480 and 960, respectively. 1, 2, 3, and 4 columns are the recovered images in the simulations (a), (b), (c), and (d), respectively

modulation system. For our method, we shift the binary modulation matrix by rows or columns or both of them. In Fig. 3b-2, c-2 are the recovered images by shifting the modulation matrix along the x axis, and the step size is the two image pixel size. In Fig. 3b-3 and c-3 are the restored images in the same situation, but the modulation matrix shift along y axis. In Fig. 3b-4, c-4, b-5, c-5 are the reconstructed images by shifting the modulation matrix with one image pixel step size along the x and y axis, respectively. In Fig. 3b-6, c-6 are the final restored images by shifting the modulation matrix along both the x and y axis with one image pixel step size. In this case, 16 kinds of shifts are performed. These results prove that our proposed method can obtain high-resolution image. The resolution of the step size determines the spatial resolution of the recovered image in ideal condition.

In the second simulation, the PSF is described as a Gaussian low-pass filter with a standard deviation of 1. For the front modulation model, the binary modulation light is affected by the PSF. Figure 4 shows an example depicting the difference between the original modulation and the degraded modulation. Owing to the effect of PSF, the modulation light illuminating the scene is degraded. In this restoration experiment, we will show the results of the

following four situations: (a) direct restoration without considering the PSF and subpixel shift; (b) restoration with considering the PSF and without subpixel shift; (c) restoration without considering the PSF and with subpixel shift; and (d) restoration with considering the PSF and with subpixel shift. When subpixel shift is taken into consideration, we shift the binary modulation matrix by rows and columns, and the step size is the one image pixel size. In Fig. 5, the first and second rows are the reconstructed results with a total sampling number of 480 and 960, respectively. In Fig. 5, the 1, 2, 3, and 4 columns show the recovered images in the situations (a), (b), (c), and (d), respectively. The PSF influences the modulation light, but the quality of the reconstructed images is degraded which can equivalent to the image filtered by the PSF. These experimental results confirm our analysis theory. When the influence of PSF is taken into consideration and subpixel shift is performed, a high-resolution image can be acquired.

For the back modulation model, because the reflected scene light is affected by the PSF, the scene information is degraded. The result is shown in Fig. 6. Four different simulations are constructed and their results are obtained, which is similar to the above experiments. The reconstructed results with the total sampling number of 480 and 960 are shown in the first and second rows of Fig. 7,1, 2, 3, and 4 columns are the restored images in the four different situations, respectively. The results show that our proposed method can also eliminate the influence of the PSF. Thus, a high-resolution image can be achieved by applying our proposed method.

4 Summary

In this paper, in order to overcome the limit of resolution in single-pixel imaging system, we propose a subpixel-shifted method to recover a high-resolution image. When the single-pixel imaging system is used in long-wave band, our method has important application prospects due to the low resolution of the image in this situation. In conclusion, the proof-of-concept has been made for the using of the subpixel shift in single-pixel imaging system and has proven to be effective. Further research is needed to study the sensitivity of this technique to the errors of the shifted and PSF parameters, and its performance in different noise scenarios.

Acknowledgments The work was supported by the National Natural Science Foundation of China (Grant Nos. 11404344, 41475001, 41205020, and 41127901).

References

1. Sun, B., Edgar, M.P., Bowman, R., Vittert, L.E., Welsh, S., Bowman, A., Padgett, M.J.: 3D computational imaging with single-pixel detectors. Science **340**, 844–847 (2013)
2. Horiuchi, N.: Computational imaging colour imaging with single-pixel detectors. Nat. Photonics **7**, 943 (2013)
3. Welsh, S.S., Edgar, M.P., Bowman, R., Jonathan, P., Sun, B.Q., Padgett, M.J.: Fast full-color computational imaging with single-pixel detectors. Opt. Express **21**, 23068–23074 (2013)
4. Howland, G.A., Lum, D.J., Ware, M.R., Howell, J.C.: Photon counting compressive depth mapping. Opt. Express **21**, 23822–23837 (2013)
5. Zhao, C.Q., Gong, W.L., Chen, M.L., Li, E.R., Wang, H., Xu, W.D., Han, S.S.: Ghost imaging lidar via sparsity constraints. Appl. Phys. Lett. **101**, 141123 (2012)
6. M. Assmann and M. Bayer, "Compressive adaptive computational ghost imaging," Sci. Rep-Uk **3** (2013)
7. Yu, W., Li, M., Yao, X., Liu, X., Wu, L., Zhai, G.: Adaptive compressive ghost imaging based on wavelet trees and sparse representation. Opt. Express **22**(6), 7133–7144 (2014)
8. Chen, J., Gong, W., Han, S.: Sub-Rayleigh ghost imaging via sparsity constraints based on a digital micro-mirror device. Phys. Lett. A **377**, 1844–1847 (2013)
9. Olivas, S.J., Rachlin, Y., Gu, L., Gardiner, B., Dawson, R., Laine, J.-P., Ford, J.E.: Characterization of a compressive imaging system using laboratory and natural light scenes. Appl. Optics **52**, 4515–4526 (2013)
10. Donoho, D.L.: Compressed sensing. IEEE Trans. Inf. Theory **52**(4), 1289–1306 (2006)
11. Duarte, M.F., Davenport, M.A., Takhar, D., Laska, J.N., Sun, T., Kelly, K.F., Baraniuk, R.G.: Single-pixel imaging via compressive sampling. IEEE Signal Process. Mag. **25**, 83–91 (2008)
12. Chan, W.L., Charan, K., Takhar, D., Kelly, K.F., Baraniuk, R.G., Mittleman, D.M.: A single-pixel terahertz imaging system based on compressed sensing. Appl. Phys. Lett. **93**, 121105 (2008)
13. Magalhães, F., Araújo, F.M., Correia, M.V., Abolbashari, M., Farahi, F.: Active illumination single-pixel camera based on compressive sensing. Appl. Optics **50**, 405–414 (2011)
14. Park, S.C., Park, M.K., Kang, M.G.: Super-resolution image reconstruction: a technical overview. Sig. Process. Mag. IEEE **20**(3), 21–36 (2003)
15. Farsiu, S., Robinson, M.D., Elad, M., et al.: Fast and robust multiframe super resolution. IEEE Trans. Image Process. **13**(10), 1327–1344 (2004)
16. Wang, Z.L., Zhu, J.B., Yan, F.X., Jia, H.: Superresolution imaging by dynamic single-pixel compressive sensing system. Opt. Eng. **52**, 063201 (2013)
17. Goodman, J.W.: Introduction to fourier optics. McGraw-Hill, New York (1996)
18. http://www.ti.com/lsds/ti/dlp/
19. M. Brookes. Matrix reference manual. [Online]. Available: http://www.ee.ic.ac.uk/hp/staff/dmb/matrix/intro.html
20. Sroubek, F., Cristóbal, G., Flusser, J.: Simultaneous super-resolution and blind deconvolution. J. Phys. Conf. Ser. **124**(1), 012048 (2008). **(IOP Publishing)**
21. http://users.ece.gatech.edu/∼justin/l1magic/